DOI: 10.15825/1995-1191-2025-1-172-182

FEATURES OF POLYURETHANE AND XENOPERICARDIAL PATCH REMODELING USING A LARGE ANIMAL MODEL AS AN EXAMPLE

E.A. Senokosova, E.S. Prokudina, R.A. Mukhamadiyarov, E.A. Velikanova, E.O. Krivkina, A.V. Mironov, E.S. Sardin, L.V. Antonova

Research Institute for Complex Issues of Cardiovascular Diseases, Kemerovo, Russian Federation

Objective: to compare the remodeling features of polyurethane (PU) and bovine pericardium (BP) patches that have been implanted in a sheep carotid artery for 6 months. **Materials and methods.** Synthetic matrices were fabricated from a 12% PU solution in chloroform by electrospinning on a Nanon-01A machine (MECC, Japan). Biological matrices made from commercially produced PU (Kem-Periplas Neo, CJSC Neocor, Russia) were used for comparison. The matrices were implanted as vascular patches into sheep carotid arteries (n = 3). Implantation period was 6 months. Via ultrasound scan, the patency of arteries bearing the implanted vascular prostheses was evaluated. After removal, the matrix samples were studied by histological examination, scanning electron microscopy and confocal microscopy. Prior to this, they had been stained with specific fluorescently labeled antibodies. The GraphPad Prism 8 application was used to process statistical data. **Results.** The sheep carotid artery wall was completely patent, with no aneurysmal dilatations, significant stenoses, and hematomas six months after the PU and BP matrices were implanted. The PU matrix was distinguished by a less pronounced connective-tissue capsule and no neointima hyperplasia; the thickness of the remodeled PU wall was 731.2 (711.5; 751.3) μm. At the same time, there was BP neointimal hyperplasia with a thickness of 627 (538; 817) μm and a remodeled wall thickness of 1723 (1693; 1772) μm. In comparison to BP, the PU matrix exhibited greater endothelialization and structural integrity. **Conclusion.** An *in vivo* study on sheep demonstrated the potential of PU matrix, a novel and effective material for vascular reconstruction, to maintain harmonious remodeling, bioinertness and structural integrity when in contact with blood. Due to its excellent elastic qualities and durability, PU is interesting both as a monocomponent and as a component of a composite material that can be used to create products for the needs of cardiovascular surgery.

Keywords: polyurethane, arterial patch, vascular prosthesis, xenopericardium, electrospinning, carotid artery.

INTRODUCTION

Cardiovascular diseases are the leading cause of death globally, and they also cause significant disability [1]. Atherosclerosis is a common disease that can affect the carotid arteries, leading to carotid artery stenosis of different degrees [2–5]. Angioplasty is the gold standard surgical treatment for hemodynamically significant carotid artery stenosis. It involves excision of the vessel area with atherosclerotic plaque and closure of the incision with primary sutures or a vascular patch. Autologous vessels and commercial flaps, such as decellularized bovine pericardium, porcine small intestinal submucosa (SIS), polytetrafluoroethylene (PTFE), and polyethylene terephthalate (Dacron), are commonly used as patches. However, these materials have several drawbacks, often failing to provide a long-term solution and necessitating repeated surgeries for patch replacement.

Autologous vessels, such as the great saphenous vein and superior thyroid artery, are considered the optimal material for patches due to their complete biocompatibility, absence of immune response, and resistance to thrombosis and restenosis. However, their use requires additional surgical intervention and may be restricted by vascular diseases or the limited availability of suitable implantation sites [6, 7].

Despite the widespread use of xenopericardial flaps, they have a significant drawback – the use of cytotoxic glutaraldehyde as a stabilizing cross-linking agent during material processing. Even with extensive washing protocols, complete removal of this toxic substance cannot be guaranteed. Additionally, glutaraldehyde has been linked to increased calcification, further compromising long-term graft viability [8].

As a result, various methods for processing and preserving xenomaterials are being developed to improve their safety and effectiveness [9–10]. Clinical trials of SIS as a patch have demonstrated minimal bleeding during implantation. However, pseudoaneurysm formation

Corresponding author: Evgeniya Senokosova. Address: 6, Bul'var Barbarasha, Kemerovo, 650002, Russian Federation. Phone: (951) 611-60-76. E-mail: sergeewa.ew@yandex.ru

was observed after six months, suggesting an imbalance between patch degradation and newly formed tissue synthesis, which could unpredictably affect SIS integrity [11].

Polymeric patches offer several advantages. Expanded PTFE has a porous structure, low thrombogenicity, and the ability to support endothelialization. Dacron is known for its high strength and resistance to overstretching [7]. However, PTFE implantation has been associated with prolonged hemostasis time, and long-term studies have reported cases of hemodynamically significant complications and ipsilateral strokes [12, 13]. Similarly, the use of Dacron patches carries risks of inflammatory reactions, infections, perioperative strokes, transient ischemic attacks, and restenosis [14–16].

The development of a novel material for angioplasty that ensures long-term patency of reconstructed blood vessels while minimizing the risks of restenosis, aneurysms, destructive changes, and inflammatory reactions remains a critical challenge. Tissue engineering approaches enable the creation of biomimetic materials using both natural and synthetic components.

For this purpose, we selected medical-grade polyurethane (PU) (TecoFlex) as the base material. PU exhibits several properties essential for vascular applications, including high tensile strength, elasticity, wear resistance, a small bend radius for tubular structures, and resistance to microbial attack and hydrolysis. Additionally, PU is biocompatible and hemocompatible, making it suitable for implantation [17].

PU has already been widely used in the manufacture of medical device components and implantable products [18, 19]. *In vitro* and *in vivo* studies have demonstrated its stability, showing no signs of biodegradation [20–22]. This resistance to degradation is expected to provide structural stability to the PU matrix during vascular remodeling, reducing the likelihood of aneurysm formation and ensuring long-term functionality within the vascular system.

According to the literature, sheep are considered the optimal large animal model for preclinical testing of tissue-engineered products for cardiovascular surgery, as they allow for the evaluation of key parameters such as patency, endothelialization, thromboresistance, and aneurysm formation at the implantation site [23].

In this study, a 3D porous non-woven matrix based on 12% PU was implanted into the carotid artery of sheep as a long-term vascular patch. The study duration was six months, during which the patency and remodeling of the PU matrix were assessed. As a comparison, a commercial bovine pericardial (BP) flap, routinely used in angioplasty at our medical center, was included in the evaluation.

This study will help to establish the suitability of PU for cardiovascular surgical products.

The study **aims** to assess the remodeling characteristics of synthetic PU vascular patches and compare them with BP patches following implantation in a sheep carotid artery over a six-month period.

MATERIALS AND METHODS

Fabrication of matrices

Synthetic PU matrices were fabricated using a 12% solution of Tecoflex EG-80A (Lubrizol Advanced Materials, USA) in chloroform (Vecton, Russia) via electrospinning on a Nanon-01A apparatus (MECC, Japan). The electrospinning parameters were set as follows: voltage 20 kV, manifold rotation speed 200 rpm, solution feed rate 0.5 mL/hour, and needle cleaning time 30 seconds. For comparison, biological matrices were obtained from commercially produced BP (Kem-Periplas Neo, CJSC "Neocor", Russia).

Matrix implantation into a sheep carotid artery

Surgical implantation of synthetic and biological matrices as vascular patches was performed on female Edilbay sheep, each weighing approximately 42–45 kg. The procedures were conducted sequentially in compliance with regulatory guidelines, including Order No. 1179 of the USSR Ministry of Health (October 10, 1993) and Order No. 267 of the Russian Ministry of Health (June 19, 2003), which outline the "Rules for conducting work using experimental animals". The study also adhered to the principles of the European Convention (Strasbourg, 1986) and the Helsinki Declaration of the World Medical Association (1996) on the humane treatment of animals. Ethical approval for the study was granted by the local ethics committee of the Research Institute for Complex Issues of Cardiovascular Diseases (protocol No. 6, dated May 4, 2023).

PU and BP matrices were implanted into a sheep carotid artery for a period of 6 months (n = 3, one sample for each patch type). The implanted patches measured 4×40 mm.

The surgical procedures were performed under general anesthesia, with anesthesia, intraoperative drug management, and postoperative drug support following previously established protocols [24]. Throughout the intervention, vital parameters were continuously monitored, including blood pressure, heart rate, and SpO_2. Mechanical ventilation was maintained with a respiratory rate of 12–15 breaths per minute, positive end-expiratory pressure (PEEP) of 7–9 mbar, tidal volume of 6–8 mL/kg, and an inspired oxygen fraction (FiO_2) of 40–60%.

The implantation procedure involved gaining access to the carotid artery, followed by systemic administration of 5000 U of heparin intravenously. The carotid artery was then clamped, and a longitudinal arteriotomy of up to 40.0 mm in length was performed.

Matrices measuring 40.0×4.0 mm were sutured into the arteriotomy defect using interrupted sutures with Prolene 6/0 thread (Ethicon, USA). Blood flow was restored according to the standard air embolism prevention protocol. The surgical wound was closed with Vicryl 2.0 thread (Ethicon, USA) and treated with BF glue. Additionally, 4000 anti-Xa IU/0.4 mL of enoxaparin sodium was administered subcutaneously, and the animal was subsequently extubated.

Assessment of patency of vessels with implanted matrices

The patency of carotid arteries with implanted matrices in sheep was assessed using ultrasound scanning with a portable, premium-class color Doppler system (M7, Mindray, China). Evaluations were conducted on postoperative days 1 and 5, followed by bi-monthly assessments until the planned endpoint of the study at 6 months.

Scanning electron microscopy

The explanted PU and BP matrix specimens, along with adjacent carotid artery sections, were fixed in 10% aqueous formalin (pH 7.4, BioVitrum, Russia). Post-fixation, dehydration with alcohols, and staining with uranyl acetate were performed as per a previously described technique [25]. The stained patch samples were embedded in Epon epoxy resin (Electron Microscopy Science, USA). The epoxy blocks were then ground and polished using a TegraPol-11 machine (Struers, USA), followed by contrast staining with Reynolds lead citrate. A carbon layer (10–15 nm) was sputtered using a vacuum sputtering system (EM ACE200, Leica). The surface structure of the samples was examined in backscattered electron mode using a Hitachi-S-3400N scanning electron microscope (Hitachi, Japan) in BSECOMP mode at an accelerating voltage of 10 kV.

Histological examination of samples

The preparation of explanted PU and BP matrix samples for histological examination followed a previously described procedure [26]. After deparaffinization, selected sections were stained with Harris hematoxylin (BioVitrum, Russia, Novosibirsk) and eosin (BioVitrum, Russia, Novosibirsk), followed by washing in running water, fixation in 96% alcohol, and clarification in o-xylene. Collagenization of the samples was assessed using Van Gieson stain, which involved sequential staining with Weigert's hematoxylin (BioVitrum, Russia, Novosibirsk) and picrofuchsin (BioVitrum, Russia, Novosibirsk). Calcium presence was identified using alizarin red S (Khimservice, Russia) and DAPI nuclear dye (Sigma-Aldrich, USA). The stained sections were mounted with Vitrogel (BioVitrum, Russia, Novosibirsk) and examined under an AXIO Imager A1 microscope (Carl Zeiss, Germany) at 100× and 200× magnification.

Confocal microscopy

For immunofluorescence analysis, slices were prepared from frozen explanted specimens using a cryotome (Microm HM 525, Thermo Scientific). These slices were fixed in 4% paraformaldehyde for 10 minutes and permeabilized with Triton-X100 solution (Sigma-Aldrich, USA) for 15 minutes. The sections were then stained with specific primary antibodies: rabbit anti-CD31 (Abcam, UK), mouse anti-alpha-smooth muscle actin (ACTA2) (Abcam, UK), rabbit anti-von Willebrand Factor (vWF, Abcam, UK), rabbit anti-collagen IV (Abcam, UK), mouse anti-collagen I (Abcam, UK), and rabbit anti-collagen III (Novus Biologicals, USA).

Following overnight incubation at 4 °C with the primary antibodies, the sections were treated with secondary antibodies for 1 hour at room temperature: donkey anti-rabbit IgG conjugated with Alexa Fluor 488 (Thermo Fisher Scientific, USA) and donkey anti-mouse IgG conjugated with Alexa Fluor 555 (Thermo Fisher Scientific, USA). At all staining stages, phosphate-buffered saline supplemented with 0.1% Tween (Sigma-Aldrich, USA) was used for washing. Autofluorescence was eliminated using an Autofluorescence Eliminator Reagent (Millipore, USA) according to the manufacturer's instructions. Cell nuclei were stained with DAPI (10 μg/mL, Sigma-Aldrich, USA) for 30 minutes.

The prepared samples were examined using a confocal laser scanning microscope LSM 700 (Carl Zeiss, Germany).

Statistical data analysis

Statistical data analysis was conducted using GraphPad Prism 8 software (GraphPad Software, USA). The distribution of the data was assessed using the Kolmogorov–Smirnov test. Results were presented as median (Me) with interquartile range (Q1; Q3). To compare differences between two independent groups, the Mann–Whitney U test was applied. Differences were considered statistically significant at a significance level of $p < 0.05$.

RESULTS

Results of PU matrix implantation in a sheep carotid artery

Ultrasound results at 6 months post-implantation of the PU matrix showed complete patency of the carotid artery. No significant aneurysmal dilatations, stenoses, or hematomas were detected (Fig. 1, a, b). Blood flow velocity in the patched vessel was measured at 75 cm/s (Fig. 1, b).

Upon visual inspection during access to the sheep carotid artery, the implanted PU matrix appeared consistent with ultrasound findings. The implantation site was moderately surrounded by a connective tissue capsule without signs of inflammation (Fig. 1, a). The PU patch exhibited no significant structural changes or aneurys-

mal dilations. Macroscopically, the PU matrix closely resembled the native carotid artery wall due to complete integration and remodeling (Fig. 1, a–c). The explant was soft and elastic.

In the transverse section of the carotid artery with the implanted patch, the PU matrix maintained a circular lumen alongside the vascular wall (Fig. 1, d). The matrix wall showed no neointimal hyperplasia and matched the thickness of the carotid artery wall (Fig. 1, d).

Histological examination revealed that the PU matrix maintained its structural integrity without signs of inflammation or calcification, both within the patch and in the surrounding tissues, indicating a low resorption rate and high biocompatibility (Fig. 2, a–d).

The PU matrix had a thickness of 343.3 (331.3; 361.2) μm. A neointima formed on the inner surface of the vessel at the site of the implanted patch, measuring 191.4 (164.3; 289.2) μm in thickness. Externally, the patch was

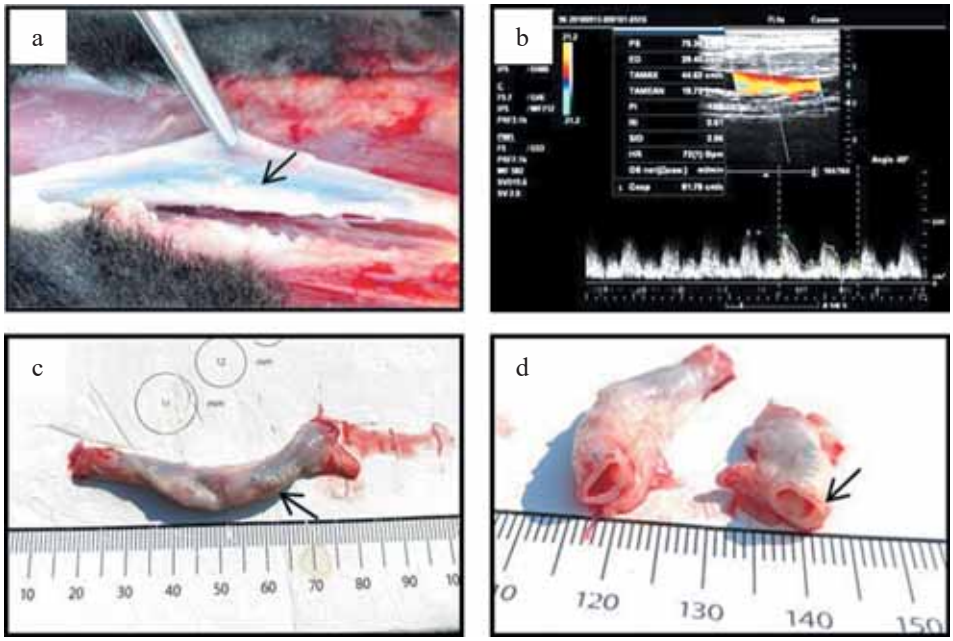

Fig. 1. PU matrix: a, view of the PU matrix 6 months after implantation in a sheep carotid artery; b, ultrasound scan image of the carotid artery 6 months after PU matrix implantation; c, explanted PU matrix with neighboring sections of the sheep carotid artery; d, cross section of the carotid artery with the implanted PU matrix

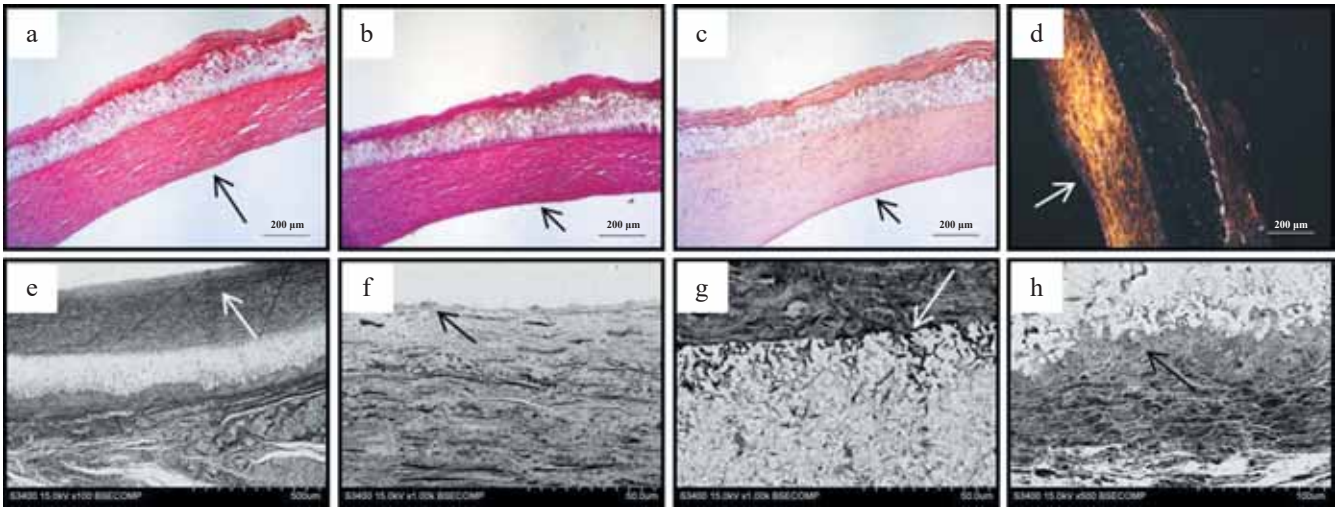

Fig. 2. Results of histological examination and scanning electron microscopy of the PU matrix 6 months after implantation into a sheep carotid artery (white and black arrows indicate neointima of the vessel): a, general view of the explanted PU matrix, H&E stain, ×50 magnification; b, general view of the PU matrix, Van Gieson's stain, ×50 magnification; c, general view of the PU matrix, alizarin red S stain, ×50 magnification; d, general view of the PU matrix, DAPI-stained fluorescence image, ×50 magnification; e, general view of the matrix, ×100 magnification; f, neointima, ×1000 magnification; g, area of junction between vessel neointima and PU matrix, ×1000 magnification; h, single foreign-body giant cells with PU fibers in the cytoplasm in the area of contact between the neoadventitia and the matrix, ×500 magnification

covered by newly formed adventitia with a thickness of 192.2 (164.0; 289.2) μm.

For comparison, the native sheep carotid artery had the following parameters: intima (20.14 (16.32; 22.70) μm; medial 530.1 (517.2; 547.7) μm; adventitia 202.6 (190.6; 212.7) μm).

Thus, remodeling of the implanted PU matrix under blood flow conditions led to the formation of both neointima and neoadventitia. The total thickness of the patched vascular wall after 6 months of implantation was 731.2 (711.5; 751.3) μm, which did not significantly differ from the native wall thickness of the sheep carotid artery (766.8 (740.4; 791.2) μm).

SEM analysis of the explanted PU matrix corroborated the histological findings, revealing no evidence of neointimal hyperplasia, inflammation, or calcification (Fig. 2, e–h). The inner vascular surface of the implanted patch was covered by a continuous layer of endothelium-like cells (Fig. 2, f). At the neointima-patch interface, macrophages were observed, with some demonstrating the ability to migrate into the matrix (Fig. 2, g).

The outer surface of the matrix was enveloped by neoadventitia, which contained histological elements characteristic of the carotid adventitial sheath, including newly formed vasa vasorum (Fig. 2, a, h). Signs of partial bioresorption were observed on the side of the implanted patch facing the neoadventitia, where the matrix was surrounded by clusters of multinucleated foreign-body giant cells (FBGCs) with isolated PU fibers detected within their cytoplasm (Fig. 2, h). Overall, monocytic-macrophage cells and multinucleated FBGCs were primarily localized in the superficial layers of the patch, while only a sparse number of cellular elements were present within the deeper regions of the PU matrix (Fig. 2, g, h).

Immunofluorescence analysis followed by confocal microscopy confirmed the presence of α-actin-producing smooth muscle-like cells within the neointima (Fig. 3, a). The inner vascular surface of the implanted PU matrix was lined by a monolayer of mature endothelial cells actively synthesizing von Willebrand factor (Fig. 3, b). Collagen III and IV were detected throughout all layers of the examined sections, including the PU matrix, neointima, and neoadventitia. However, the most intense fluorescence of these proteins was observed in the endothelial layer (Fig. 3, c, d). Cellular infiltration within the PU matrix remained low.

Consequently, the remodeling of the PU matrix implanted into a sheep carotid artery over a 6-month period led to the development of a three-layer structure resembling the native vascular wall. The absence of premature material degradation, calcification, inflammation, aneurysmal formation, or stenotic changes highlights the high biocompatibility of PU as a vascular patch material.

Results of BP matrix implantation in a sheep carotid artery

Ultrasound evaluation at 6 months post-implantation of the BP matrix in a sheep carotid artery confirmed vessel patency, with no evidence of aneurysmal dilatation, stenosis, or significant hematomas. The blood flow velocity at the site of the implanted patch averaged 67 cm/s (Fig. 4, a, b).

Upon visual inspection during access to the sheep carotid artery, no significant structural changes, aneurysmal dilatations, or hematomas were observed at the BP matrix implantation site (Fig. 4, a). A vascularized connective tissue capsule uniformly enveloped the implanted BP matrix (Fig. 4, a, c). The explant remained elastic with a dense structure.

A transverse section of the carotid artery confirmed that the BP matrix maintained a circular lumen in combination with the vascular wall (Fig. 4, d). However, the implanted patch site appeared thicker than the native carotid artery wall, which may indicate neointimal hyperplasia (Fig. 4, d).

Histological analysis of the explanted BP matrix confirmed that its structural integrity was largely preserved after 6 months of implantation (Fig. 5, a–d). However, minor areas of delamination were observed within the

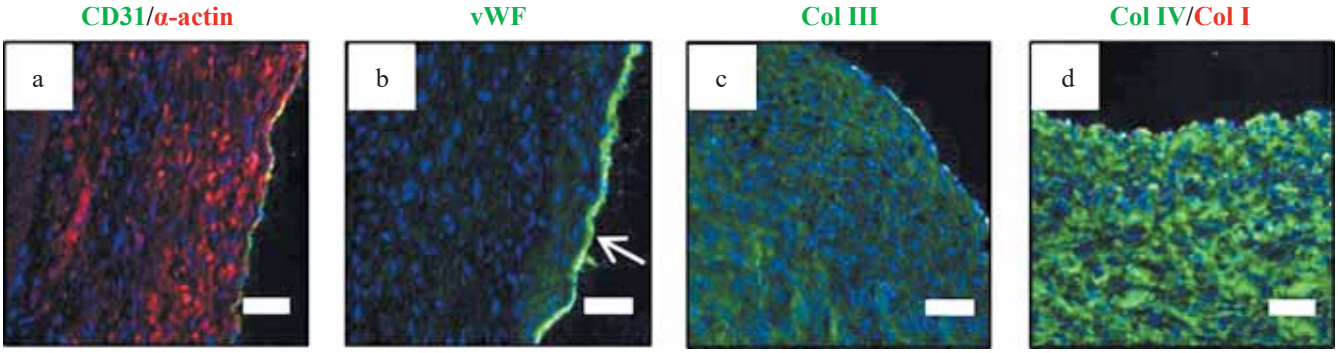

Fig. 3. Results of immunofluorescence study of PU matrix 6 months after implantation in a sheep carotid artery, ×200 magnification, scale bar 50 μm: a, endothelium on the inner surface (CD31, green glow), alpha actin-containing cells (red glow); b, von Willebrand factor (vWF, green glow); c, collagen type III (Col III, green glow); d, collagen type IV (Col IV, green glow), collagen type I (Col I, red glow), DAPI-stained cell nuclei (blue glow)

patch, though these did not significantly affect its overall architecture (Fig. 5, a–d). No signs of calcification or inflammation were detected.

By the end of the 6-month implantation period, remodeling of the BP matrix led to the formation of a neointima with a thickness of 627 (538; 817) μm and a neoadventitia with an average thickness of 540 (504; 540) μm. The total vascular wall thickness at the implantation site measured 1723 (1693; 1772) μm, nearly twice the thickness of the intact carotid artery wall (869 (833; 875) μm), indicating the presence of neointimal hyperplasia in the patched region.

A detailed examination of the explanted BP matrix confirmed the absence of inflammation and calcification (Fig. 5, e–h). The inner vascular surface was lined with a loose layer of endothelial-like cells (Fig. 5, e–g). Single areas of delamination were observed at the BP matrix implantation site, but these did not compromise the overall structural integrity of the patch (Fig. 5, e–f). The neointima exhibited a tendency to thicken, both centrally and

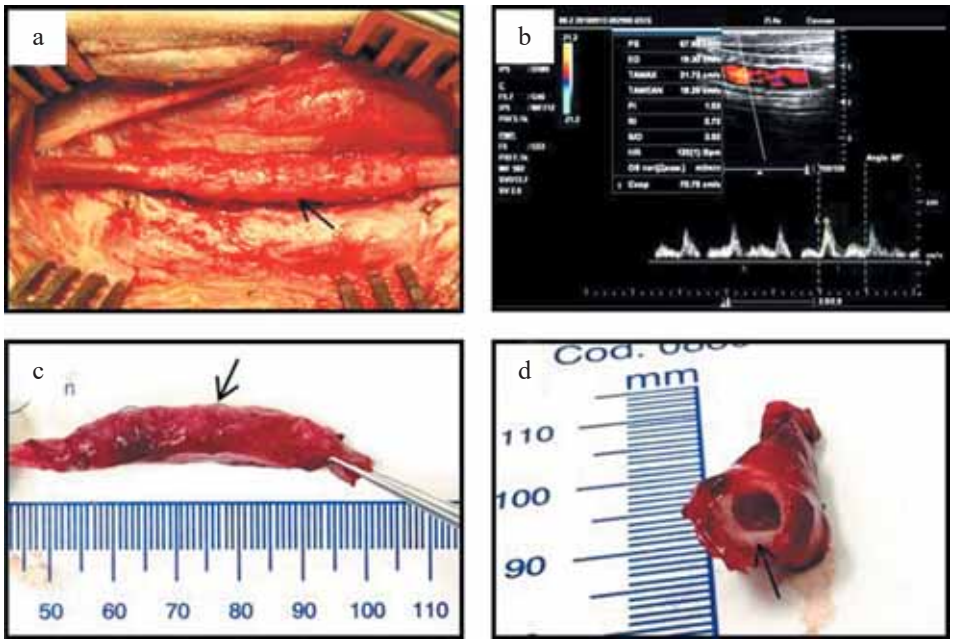

Fig. 4. BP matrix: a, view of the BP matrix 6 months after implantation in a sheep carotid artery; b, ultrasound scan of the carotid artery 6 months after implantation of the BP matrix; c, explanted section of the carotid artery with the implanted BP matrix; d, cross section of the carotid artery with the implanted BP matrix

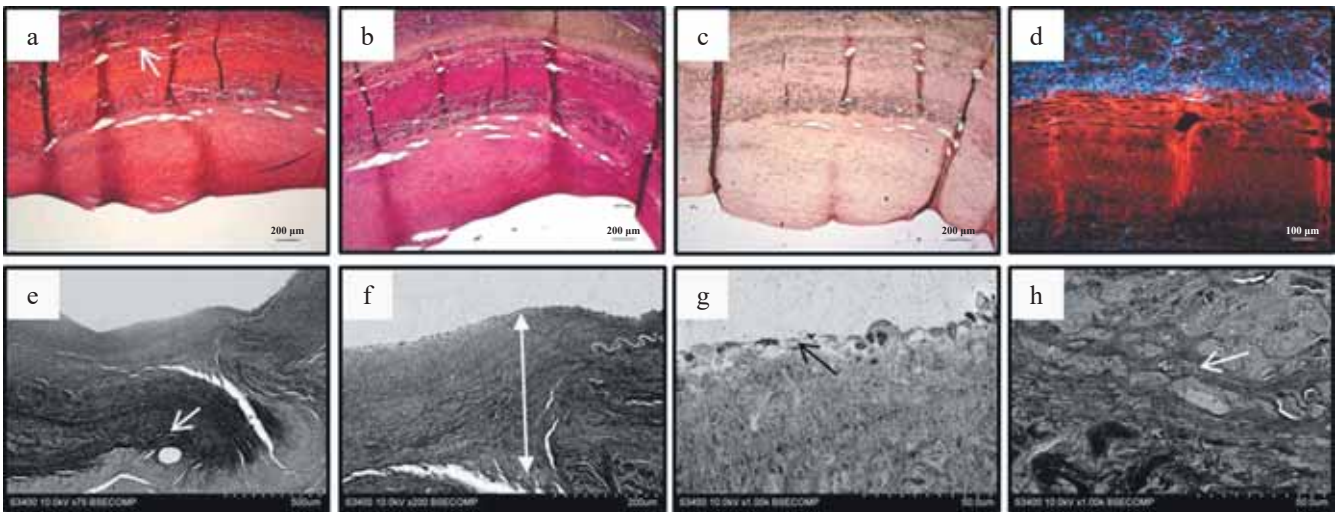

Fig. 5. Results of histologic examination and scanning electron microscopy of the BP matrix 6 months after implantation into a sheep carotid artery: a, general view of the BP matrix, H&E stain, ×50 magnification; b, general view of the BP matrix, Van Gieson's stain, ×50 magnification; c, general view of the BP matrix, alizarin red C color, ×50 magnification; d, general view of the BP matrix, DAPI-stained fluorescence image, ×100 magnification; e, general view of the matrix, ×75 magnification; f, area of anastomosis, ×200 magnification; g, vessel neointima, magnification ×1000; h, single foreign-body giant cells in the area of contact between the neoadventitia and the matrix, ×1000 magnification

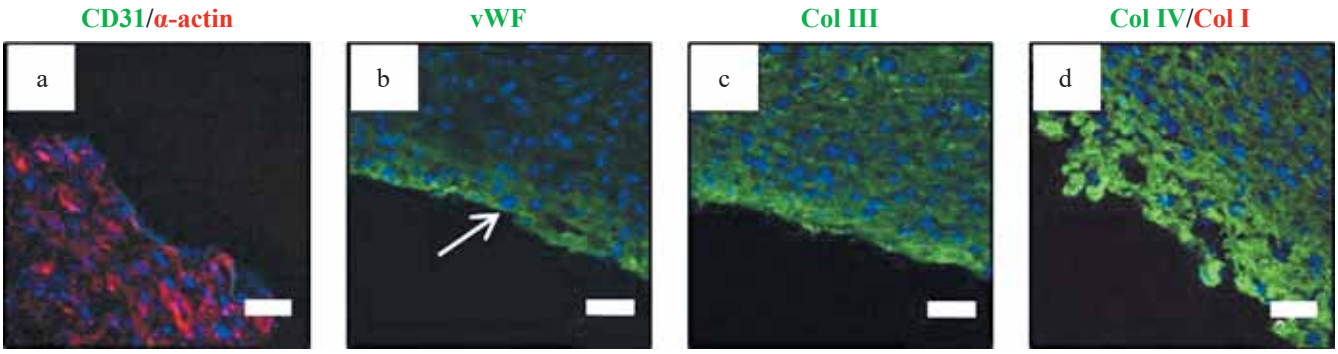

Fig. 6. Results of immunofluorescence study of the BP matrix 6 months after implantation in a sheep carotid artery, ×200 magnification, scale bar 50 μm: a, endothelium on the inner surface (CD31, green glow), alpha actin-containing cells (red glow); b, von Willebrand factor (vWF, green glow); c, collagen type III (Col III, green glow); d, collagen type IV (Col IV, green glow), collagen type I (Col I, red glow), DAPI-stained cell nuclei (blue glow)

in the anastomotic regions (Fig. 5, e–f). The implanted xenopericardial flap retained the fibrous structure characteristic of bovine pericardium (Fig. 5, e). While the cellularity of the patch was low, single multinucleated foreign-body giant cells (FBGCs) were detected at the interface with the neoadventitia (Fig. 5, h).

Immunofluorescence analysis of the explanted BP matrix revealed the presence of squamous alpha-actin-producing cells within the neointima (Fig. 6, a). The endothelial layer lining the inner vascular surface appeared loose and discontinuous, with weak expression of von Willebrand factor (Fig. 6, b). Collagen III fibers were detected throughout all layers of the sample, including the neointima, matrix, and neoadventitia (Fig. 6, c). Collagen IV was present in all layers, with individual brightly stained secreting cells scattered throughout (Fig. 6, d).

Thus, remodeling of the BP matrix implanted in a sheep carotid artery followed the process of forming a tissue analog of the vascular wall, comprising both neointima and neoadventitia. A key distinguishing feature of the biological patch was the presence of localized delamination, indicative of material degradation. Additionally, the pronounced neointimal hyperplasia observed after six months of implantation highlights structural and functional differences between the implanted BP matrix and the native carotid artery wall.

DISCUSSION

Commercial grafts used for vascular reconstruction present several unresolved challenges, including thrombosis, calcification, neointimal hyperplasia, and aneurysm formation [27, 28]. Beyond these issues, xenopericardial grafts are particularly susceptible to structural degeneration, especially in younger individuals [29, 30]. Materials such as PTFE and Dacron have also been associated with calcium deposition, not only within the graft itself but also in adjacent vascular structures, including the adventitia, media, and intima [31].

Neointimal hyperplasia remains a critical concern in vascular surgery, as it significantly impacts the long-term success of both surgical and endovascular procedures [32]. In our previous *in vitro* studies, we demonstrated that a PU material exhibited favorable physical and mechanical properties, with the potential to mitigate neointimal hyperplasia. Notably, PU showed lower stiffness compared to xenopericardium [33].

Our in-house study on a novel vascular patch material composed of 12% electrospun PU in a long-term sheep carotid artery implantation model demonstrated several advantages over commercial BP.

A key distinction between the two materials was observed visually at the time of explantation. The connective tissue capsule surrounding the BP patch was denser compared to PU. Cross-sectional analysis further revealed a seamless integration of PU with the arterial wall, whereas BP exhibited pronounced thickening, indicating structural disparity.

Secondly, histological evaluation confirmed the absence of neointimal hyperplasia in the PU matrix and a closer resemblance to the native artery. The total thickness of the remodeled PU vascular wall was 731.2 (711.5; 751.3) μm, aligning well with the native carotid artery. In contrast, BP demonstrated significant neointimal hyperplasia (627 (538; 817) μm thick), resulting in an overall vascular wall thickness of 1723 (1693; 1772) μm after six months of implantation.

Thirdly, the endothelial lining on the PU matrix was more continuous and functionally active compared to the less-developed endothelialization observed in BP.

Fourthly, the structural integrity of PU was higher than that of BP. While multinucleated FBGCs were present at the neoadventitia border in both materials, the location of these cells in BP was the same, but the material was stratified.

Despite both materials supporting 100% patency of the reconstructed carotid arteries and maintaining physiological blood flow over the six-month implantation period without aneurysm formation, the PU-based matrix demonstrated superior remodeling capabilities under hemodynamic conditions. Given these advantages, PU

shows strong potential for use as a standalone component or as part of a composite structure to enhance elasticity and durability in vascular reconstruction applications.

CONCLUSION

The implantation of a PU matrix as a vascular patch demonstrated harmonious remodeling and preservation of the polymer framework under physiological blood flow conditions in a sheep model. Its high elasticity and durability make PU a promising material for cardiovascular surgical applications, either as a standalone component or as part of a composite structure designed to enhance vascular reconstruction outcomes.

This research was conducted as part of the fundamental theme of the Research Institute for Complex Issues of Cardiovascular Diseases, No. 0419-2022-0001: "Molecular, cellular, and biomechanical mechanisms of the pathogenesis of cardiovascular diseases in the development of new treatment methods for cardiovascular diseases based on personalized pharmacotherapy, minimally invasive medical devices, biomaterials, and tissue-engineered implants".

The authors declare no conflict of interest.

REFERENCES

1. *Virani SS, Alonso A, Benjamin EJ, Bittencourt MS, Callaway CW, Carson AP et al*. Heart Disease and Stroke Statistics-2020 Update: A Report From the American Heart Association. *Circulation*. 2020; 141 (9): e139–e596. doi: 10.1161/CIR.0000000000000757.
2. *Feigin VL, Brainin M, Norrving B, Martins S, Sacco RL, Hacke W et al.* World Stroke Organization (WSO): Global Stroke Fact Sheet 2022. *Int J Stroke.* 2022; 17 (1): 18–29. doi: 10.1177/17474930211065917.
3. *Pashneh-Tala S., MacNeil S., Claeyssens F.* The Tissue-Engineered Vascular Graft-Past, Present, and Future. *Tissue Eng Part B Rev.* 2016; 22 (1): 68–100. doi: 10.1089/ten.teb.2015.0100.
4. *Benjamin EJ, Muntner P, Alonso A, Bittencourt MS, Callaway CW, Carson AP et al.* Heart Disease and Stroke Statistics-2019 Update: A Report From the American Heart Association. *Circulation.* 2019; 139 (10): 56–528. doi: 10.1161/CIR.0000000000000659.
5. *Roth GA, Mensah GA, Johnson CO, Addolorato G, Ammirati E, Baddour LM et al.* Global Burden of Cardiovascular Diseases and Risk Factors, 1990–2019: Update From the GBD 2019 Study. *J Am Coll Cardiol*. 2020; 76 (25): 2982–3021. doi: 10.1016/j.jacc.2020.11.010.
6. *Yarikov AV, Balyabin AV, Yashin KS, Mukhin AS.* Surgical Treatment Modalities of Carotid Artery Stenosis (Review). *Modern Technologies in Medicine*. 2015; 7 (4): 189–200. doi: 10.17691/stm2015.7.4.25.
7. *Muto A, Nishibe T, Dardik H, Dardik A.* Patches for carotid artery endarterectomy: current materials and prospects. *J Vasc Surg.* 2009; 50 (1): 206–213. doi: 10.1016/j.jvs.2009.01.062.
8. *Chernyavskiy AM, Larionov PM, Stolyarov MS, Starodubtsev VB.* Structural transformation of xenopericardium after implantation into the carotid artery (prospective study). *Pathology of blood circulation and cardiac surgery*. 2007; 4: 37–40.
9. *Kudryavtseva Yu.A.* Bioprosthetic heart valves. From idea to clinical use. *Complex Issues of Cardiovascular Diseases*. 2015; (4): 6–16. (In Russ.). doi: 10.17802/2306-1278-2015-4-6-16.
10. *Rezvova MA, Ovcharenko EA, Glushkova TV, Kudryavtseva YuA, Barbarash LS.* Evaluation of calcification resistance of xenopericardium treated with polyhydroxy compounds. *Russian Journal of Transplantology and Artificial Organs*. 2021; 23 (1): 75–83. doi: 10.15825/1995-1191-2021-1-75-83.
11. *Weber SS, Annenberg AJ, Wright CB, Braverman TS, Mesh CL.* Early pseudoaneurysm degeneration in biologic extracellular matrix patch for carotid repair. *J Vasc Surg.* 2014; 59 (4): 1116–1118. doi: 10.1016/j.jvs.2013.05.012.
12. *Fokin AA, Kuvatov AV.* Remote results of carotid artery reconstructions using a patch. *Journal of Experimental and Clinical Surgery*. 2013; 6 (2): 239–243.
13. *Ren S, Li X, Wen J, Zhang W, Liu P.* Systematic review of randomized controlled trials of different types of patch materials during carotid endarterectomy. *PLoS One.* 2013; 8 (1): e55050. doi: 10.1371/journal.pone.0055050.
14. *Alawy M, Tawfick W, ElKassaby M, Shalaby A, Zaki M, Hynes N, Sultan S.* Late Dacron Patch Inflammatory Reaction after Carotid Endarterectomy. *Eur J Vasc Endovasc Surg.* 2017; 54 (4): 423–429. doi: 10.1016/j.ejvs.2017.06.015.
15. *Xu JH, Altaf N, Tosenovsky P, Mwipatayi BP.* Management challenges of late presentation Dacron patch infection after carotid endarterectomy. *BMJ Case Rep.* 2017; 2017: bcr2017221541. doi: 10.1136/bcr-2017-221541.
16. *Rerkasem K, Rothwell PM.* Systematic review of randomized controlled trials of patch angioplasty versus primary closure and different types of patch materials during carotid endarterectomy. *Asian J Surg.* 2011; 34 (1): 32–40. doi: 10.1016/S1015-9584(11)60016-X.
17. *Kucinska-Lipka J, Gubanska I, Janik H, Sienkiewicz M.* Fabrication of polyurethane and polyurethane based composite fibres by the electrospinning technique for soft tissue engineering of cardiovascular system. *Mater Sci Eng C Mater Biol Appl.* 2015; 46: 166–176. doi: 10.1016/j.msec.2014.10.027.
18. *LaPorte RJ.* Hydrophilic polymer coatings for medical devices. *Routledge.* 2017; 11–16. doi: 10.1201/9780203751381.
19. *Kheradvar A, Groves EM, Dasi LP, Alavi SH, Tranquillo R, Grande-Allen KJ et al.* Emerging trends in heart valve engineering: Part I. Solutions for future. *Ann Biomed Eng*. 2015; 43 (4): 833–843. doi: 10.1007/s10439-014-1209-z.
20. *Bergmeister H, Grasl C, Walter I, Plasenzotti R, Stoiber M, Schreiber C et al.* Electrospun small-diameter polyurethane vascular grafts: ingrowth and differentiation of vascular-specific host cells. *Artif Organs.* 2012; 36 (1): 54–61. doi: 10.1111/j.1525-1594.2011.01297.x.

21. *Grasl C, Bergmeister H, Stoiber M, Schima H, Weigel G.* Electrospun polyurethane vascular grafts: *in vitro* mechanical behavior and endothelial adhesion molecule expression. *J Biomed Mater Res A.* 2010; 93 (2): 716–723. doi: 10.1002/jbm.a.32584.
22. *Bergmeister H, Schreiber C, Grasl C, Walter I, Plasenzotti R, Stoiber M et al.* Healing characteristics of electrospun polyurethane grafts with various porosities. *Acta Biomater*. 2013; 9 (4): 6032–6040. doi: 10.1016/j.actbio.2012.12.009.
23. *Schleimer K, Jalaie H, Afify M, Woitok A, Barbati ME, Hoeft K et al.* Sheep models for evaluation of novel patch and prosthesis material in vascular surgery: tips and tricks to avoid possible pitfalls. *Acta Vet Scand*. 2018; 60 (1): 42. doi: 10.1186/s13028-018-0397-1.
24. *Antonova LV, Mironov AV, Yuzhalin AE, Krivkina EO, Shabaev AR, Rezvova MA et al.* A Brief Report on an Implantation of Small-Caliber Biodegradable Vascular Grafts in a Carotid Artery of the Sheep. *Pharmaceuticals (Basel).* 2020 May 21; 13 (5): 101. doi: 10.3390/ph13050101.
25. *Antonova L, Kutikhin A, Sevostianova V, Lobov A, Repkin E, Krivkina E et al.* Controlled and Synchronised Vascular Regeneration upon the Implantation of Iloprost- and Cationic Amphiphilic Drugs-Conjugated Tissue-Engineered Vascular Grafts into the Ovine Carotid Artery: A Proteomics-Empowered Study. *Polymers (Basel).* 2022 Nov 26; 14 (23): 5149. doi: 10.3390/polym14235149.
26. *Antonova L, Kutikhin A, Sevostianova V, Velikanova E, Matveeva V, Glushkova T et al.* bFGF and SDF-1α Improve *In Vivo* Performance of VEGF-Incorporating Small-Diameter Vascular Grafts. *Pharmaceuticals (Basel)*. 2021 Mar 28; 14 (4): 302. doi: 10.3390/ph14040302.
27. *Terakawa K, Yamauchi H, Lee Y, Ono M.* A Novel Knitted Polytetrafluoroethylene Patch for Cardiovascular Surgery. *Int Heart J.* 2022; 63 (1): 122–130. doi: 10.1536/ihj.21-564.
28. *Liesker DJ, Gareb B, Looman RS, Donners SJA, de Borst GJ, Zeebregts CJ, Saleem BR.* Patch angioplasty during carotid endarterectomy using different materials has similar clinical outcomes. *J Vasc Surg.* 2023; 77 (2): 559–566.e1. doi: 10.1016/j.jvs.2022.09.027.
29. *Aguiari P, Fiorese M, Iop L, Gerosa G, Bagno A.* Mechanical testing of pericardium for manufacturing prosthetic heart valves. *Interact Cardiovasc Thorac Surg*. 2016; 22 (1): 72–84. doi: 10.1093/icvts/ivv282.
30. *Fadeeva IS, Sorkomov MN, Zvyagina AI, Britikov DV, Sachkov AS, Evstratova YaV et al.* Study of Biointegration and Elastic-Strength Properties of a New Xenopericardium-Based Biomaterial for Reconstructive Cardiovascular Surgery. *Bull Exp Biol Med.* 2019; 167 (4): 496–499. doi: 10.1007/s10517-019-04558-1.
31. *Lejay A, Bratu B, Kuntz S, Neumann N, Heim F, Chakfé N.* Calcification of Synthetic Vascular Grafts: A Systematic Review. *EJVES Vasc Forum.* 2023; 29 (60): 1–7. doi: 10.1016/j.ejvsvf.2023.05.013.
32. *Collins MJ, Li X, Lv W, Yang C, Protack CD, Muto A et al.* Therapeutic strategies to combat neointimal hyperplasia in vascular grafts. *Expert Rev Cardiovasc Ther.* 2012; 10 (5): 635–647. doi: 10.1586/erc.12.33.
33. *Senokosova EA, Prokudina ES, Matveeva VG, Velikanova EA, Glushkova TV, Koshelev VA et al.* Tissue engineering matrix based on polyurethane: *in vitro* research. *Complex Issues of Cardiovascular Diseases.* 2023; 12 (4S): 120–130. [In Russ.]. doi: 10.17802/2306-1278-2023-12-4S-120-130.

The article was submitted to the journal on 19.03.2024